ECCOMAS Thematic Conference on Multibody Dynamics
July 24 - 28, 2023, Lisbon, Portugal

Pushing manipulation with a Nonholonomic Mobile Base

Yujie Tang, Martijn Wisse

Department of Cognitive Robotics
Delft University of Technology
Mekelweg 2, 2628 CD Delft, The Netherlands
{Y.Tang-6, M.Wisse}@tudelft.nl

EXTENDED ABSTRACT

1 Introduction

Mobile manipulators have potential for practical applications, such as in logistics operations, but require the ability to handle objects too large for their arm(s). This can be achieved through endowing the robot with the capability to push objects to a desired location. Previous studies have attempted pushing manipulation using the robot arm, but this approach is limited by the arm's payload capacity. Our paper focuses on using the more capable mobile base for pushing instead. We consider a goal-conditioned pushing planning problem using a cylinder-shaped differential-drive robot to push a polygonal object, as depicted in Figure. 1c, 1d. There are two key challenges in previous pushing planning studies: 1) the discontinuity of the contact dynamics, which hinders planning and control, and 2) the commonly used planar pushing model that disregards the shape of the robot and ignores the relative motion between the robot and pushed object [1, 2]. Our objective is to develop a continuous dynamics model for mobile pushing and demonstrate its use in pushing control.

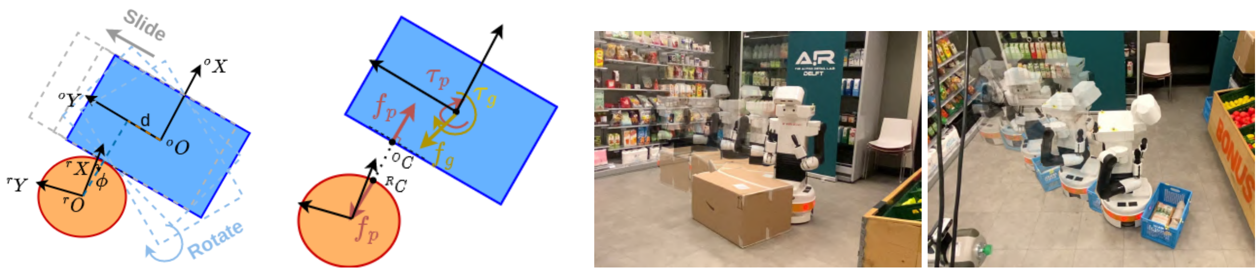

(a) (b) (c) (d)

Figure 1: (a) and (b) show the model of the robot-object system under pushing. (c) and (d) present the pushing control result based on the proposed robot-object model with a Tiago robot.

2 Dynamics Model for Robot Pushing

Friction-less Continuous Robot-Object Contact. The physical interaction between the robot and the object during the pushing process can be modeled as a 2D constrained multibody dynamics problem, as depicted in Figure. 1a and 1b. Instead of categorizing the robot-object contact modes into discrete states as in previous studies [1, 2], we assume frictionless contact between the robot and the pushed object. For simplification, a contact constraint is imposed to maintain continuous contact and prevent transition to the separation mode. The robot is also constrained to prevent backward motion and deceleration that exceeds the object's deceleration from floor friction. The contact constraint is summarized as:

$$^{\mathscr{R}}v_{\mathrm{r}} > 0,\ -90^\circ < \phi < 90^\circ, \text{ and } |acc_{\mathrm{r}}| < acc_{\mathrm{r,\,max}}. \tag{1}$$

where $^{\mathscr{R}}v_{\mathrm{r}}$ is the linear velocity of the robot [1], ϕ denotes the angle between the object and the robot frame as shown in Fig. 1a, acc_{r} is the acceleration of the robot, $acc_{\mathrm{r,\,max}}$ is the maximum acceleration of the robot.

Continuous friction model for object-ground contact. A continuous (i.e., non-Coulomb) friction model is used to mathematically approximate the Coulomb's law of friction such that the contact dynamics can be modeled in a continuous fashion. We assume the friction interaction between the object and the ground at the contact surface with a constant coefficient of friction, μ_{g}. The friction force at position $^{\mathscr{W}}\mathrm{p}$ is expressed as

$$\mathbf{f}_{\mathrm{g},\mathbf{p}} = -\mu_{\mathrm{g}} \cdot (2\mathrm{sig}(\mathbf{v}_{\mathrm{p}}) - 1) \cdot f_{\mathrm{n}} \tag{2}$$

where f_{n} is the normal force at $^{\mathscr{W}}\mathrm{p}$, $\mathbf{v}_{\mathrm{p}} = [\dot{x}_{\mathrm{o}}, \dot{y}_{\mathrm{o}}]^{\mathrm{T}}$ the velocity of $^{\mathscr{W}}\mathrm{p}$ expressed in the world frame, μ_{g} the friction coefficient, and $\mathrm{sig}(\cdot) = \frac{1}{1+exp(-(\cdot))}$ the sigmoid function.

Multibody dynamics model for the pushing system. Since we assume (and control) that the contact between the robot and the object is carefully maintained, the robot-object system is modeled as two rigid bodies connected by an idealized sliding joint. The

[1]The superscript $\mathscr{R}$ denotes the Robot frame. The Object and the World frame are respectively represented as $\mathscr{O}$ and $\mathscr{W}$. $\mathscr{W}$ is always omitted for simplicity.

mobile robot is assumed to be controlled in a closed loop to achieve the desired movement, so its motion will not be influenced by the reaction force exerted by the object. For the pushed object, its motion is a result of the contact interaction with the robot. The dynamics of the object can be achieved by a combination of the Newton-Euler equations of motion and a contact constraint equation in the form of Differential Algebraic Equations. The Newton Euler equations of motion for the object are,

$$\begin{cases} \cos(\theta_o)^{\mathscr{O}} f_{\mathrm{x,p}} + f_{\mathrm{x,f}} = m_{\mathrm{o}}\ddot{x}_{\mathrm{o}} \\ \sin(\theta_o)^{\mathscr{O}} f_{\mathrm{x,p}} + f_{\mathrm{y,f}} = m_{\mathrm{o}}\ddot{y}_{\mathrm{o}} \\ -^{\mathscr{O}} y_{\mathrm{c}}{}^{\mathscr{O}} f_{\mathrm{x,p}} + \tau_{\mathrm{f}} = I_{\mathrm{o}}\ddot{\theta}_{\mathrm{o}} \end{cases} \tag{3}$$

where $\mathbf{x}_{\mathrm{o}} = [x_{\mathrm{o}}, y_{\mathrm{o}}, \theta_{\mathrm{o}}]^T \in \mathbb{R}^3$ denote the robot's state vector, $x_{\mathrm{o}}, y_{\mathrm{o}}$ are the position of the robot in the World frame, θ_{o} is its orientation. ${}^{\mathscr{O}} f_{\mathrm{x,p}}$ is the x-component of the push force in the Object frame. $f_{\mathrm{x,f}}$ is the x-component of the friction force exerted by the ground in the World frame. ${}^{\mathscr{O}} y_c$ is the position of the contact point in y direction of the Object frame, m_{o} and I_{o} are the mass and moment of inertia of the object.

Since the robot and the object always keep contact, the contact constraint can be expressed as ${}^{\mathscr{O}} x_{\mathrm{r}} = \cos(\theta_{\mathrm{o}})(x_{\mathrm{r}} - x_{\mathrm{o}}) + \sin(\theta_{\mathrm{o}})(y_{\mathrm{r}} - y_{\mathrm{o}}) = -r_{\mathrm{r}} - \frac{1}{2}W_{\mathrm{o}}$, where $r_{\mathrm{r}}, W_{\mathrm{o}}$ respectively denote the radius of the robot and the width of the object. By differentiating the contact constraint twice with respect to time, we can achieve the constraint on the object accelerations:

$$C_{,\mathbf{x}} * \ddot{\mathbf{x}}_{\mathrm{r}} + \mathbf{g}_{,\mathbf{x}} = 0 \tag{4}$$

with $\mathbf{g}_{,\mathbf{x}} = -\cos(\theta_{\mathrm{o}})\dot{\theta}_{\mathrm{o}}\dot{\theta}_{\mathrm{o}}(x_{\mathrm{r}} - x_{\mathrm{o}}) + \cos(\theta_{\mathrm{o}})\ddot{x}_{\mathrm{r}} + \sin(\theta_{\mathrm{o}})\ddot{y}_{\mathrm{r}} - 2\sin(\theta_{\mathrm{o}})\dot{\theta}_{\mathrm{o}}(\dot{x}_{\mathrm{r}} - \dot{x}_{\mathrm{o}}) - \sin(\theta_{\mathrm{o}})\dot{\theta}_{\mathrm{o}}\dot{\theta}_{\mathrm{o}}(y_{\mathrm{r}} - y_{\mathrm{o}}) + 2\cos(\theta_{\mathrm{o}})\dot{\theta}_{\mathrm{o}}(\dot{y}_{\mathrm{r}} - \dot{y}_{\mathrm{o}})$, and matrix $C_{,\mathbf{x}} = [-\cos(\theta_{\mathrm{o}}), -\sin(\theta_{\mathrm{o}}), -\sin(\theta_{\mathrm{o}})(x_{\mathrm{r}} - x_{\mathrm{o}}) + \cos(\theta_{\mathrm{o}})(y_{\mathrm{r}} - y_{\mathrm{o}})]$.

Combining the equations of motion Eq. 3 and the contact constraint equation Eq. 4 leads to a full set of DAEs:

$$\begin{bmatrix} M & C_{,\mathbf{x}}^{\mathrm{T}} \\ C_{,\mathbf{x}} & 0 \end{bmatrix} \begin{bmatrix} \ddot{\mathbf{x}}_{\mathrm{o}} \\ {}^{\mathscr{O}} f_{\mathrm{x,p}} \end{bmatrix} = \begin{bmatrix} \mathbf{w}_{\mathrm{g}} \\ \mathbf{g}_{,\mathbf{x}} \end{bmatrix} \tag{5}$$

where $M = \mathrm{diag}[m_{\mathrm{o}}, m_{\mathrm{o}}, I_{\mathrm{o}}]$, and $\mathbf{w}_{\mathrm{g}} = [f_{\mathrm{x,g}}, f_{\mathrm{y,g}}, \tau_{\mathrm{g}}]^{\mathrm{T}}$ is the wrench exerted by the ground.

3 Result and Conclusion

We assess the validity of the proposed pushing dynamics model through real-world experiments, utilizing a Tiago robot to push a 1.5 kg box with dimensions of $0.565 \times 0.755 \times 0.425$ m^3 and ground-box friction coefficient of $\mu_{\mathrm{g}} = 0.4$. Control commands, as well as pose and twist data for the robot and object, were collected for 2 minutes with a sampling time of $\delta t = 0.1$ s. The proposed contact dynamics models were then applied to predict the motion of the object, as depicted in Fig. 2.

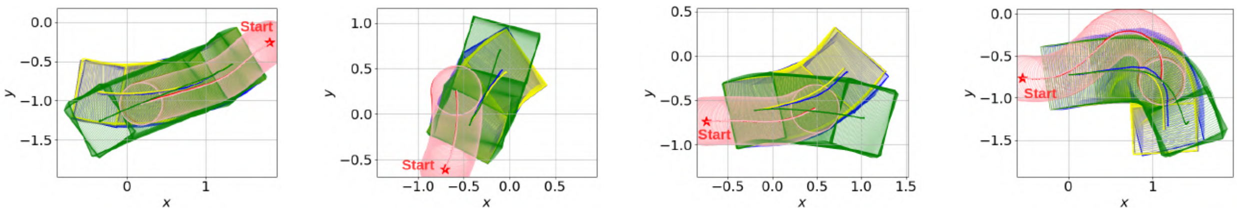

(a) Trail 1 (b) Trail 2 (c) Trail 3 (d) Trail 4

Figure 2: The measured and predicted trajectory of the robot and the object under pushing manipulation. The red and blue trajectories respectively denote the measured robot and object trajectory from the motion capture system. The pink trajectory is the predicted robot trajectory with the robot motion model. The yellow and green ones are respectively object trajectories predicted by the DAE model (Eq. 5), and the pushing model with simplified friction calculation.

It is important to point out that the friction force exerted by the ground is calculated by integrating the force over the contact patch. Accurate integration requires a long solution time which can not be achieved in real-time control. So we simplify the integration by only summing for the force at the corners of the polygonal object. The trajectory predicted by the simplified model is shown as the green trajectory in Figure. 2. With the simplified dynamics model of the pushing system, we formulate the goal-conditioned pushing planning problem as an Optimal Control Problem. We apply the pushing controller to the Tiago robot to push large and heavy objects, whose result is shown in Figure. 1c and 1d. Transparency of the robot and objects indicates their movement. As we can see from the figures, the controller can successively achieve the pushing task by pushing the object to the goal location while maintaining contact with the objects. A detailed description of the full algorithm as well as the results will be presented in the full paper.

References

[1] Hogan FR, Rodriguez A. Reactive planar non-prehensile manipulation with hybrid model predictive control. The International Journal of Robotics Research. 2020;39(7):755-773. doi:10.1177/0278364920913938

[2] Moura, João, Theodoros Stouraitis, and Sethu Vijayakumar. "Non-prehensile planar manipulation via trajectory optimization with complementarity constraints." 2022 International Conference on Robotics and Automation (ICRA). IEEE, 2022.